4. Wolpoff, M., Senut, B., Pickford, M. & Hawks, J. *Sahelanthropus* or '*Sahelpithecus*'? *Nature* **419,** 581–582 (2002).
5. Brunet, M. *et al. Sahelanthropus* or '*Sahelpithecus*'? (Reply). *Nature* **419,** 582 (2002).
6. Vignaud, P. *et al.* Geology and palaeontology of the Upper Miocene Toros-Menalla hominid locality, Djurab Desert, Northern Chad. *Nature* **418,** 152–155 (2002).
7. Brunet, M. *et al.* Tchad: un nouveau site à Hominidés Pliocène. *C. R. Acad. Sci. Paris* **324,** 341–345 (1997).
8. Deino, A. L., Tauxe, L., Monaghan, M. & Hill, A. Ar^{40}/Ar^{39} geochronology and paleomagnetic stratigraphy of the Lukeino and lower Chemeron Formations at Tabarin and Kapcheberek, Tugen Hills, Kenya. *J. Hum. Evol.* **42,** 117–140 (2002).
9. MacDougall, I. & Feibel, C. in *Lothagam the Dawn of Humanity in Eastern Africa* (eds Leakey, M. G. & Harris, J. M.) 43–64 (Columbia University Press, New York, 2003).
10. Haile-Selassie, Y., Suwa, G. & White, T. Late Miocene teeth from Middle Awash, Ethiopia, and early hominid dental evolution. *Science* **303,** 1503–1505 (2004).
11. Haile-Selassie, Y. Late Miocene hominids from the Middle Awash, Ethiopia. *Nature* **412,** 178–181 (2001).
12. White, T. D., Suwa, G. & Asfaw, B. *Australopithecus ramidus*, a new species of hominid from Aramis, Ethiopia. *Nature* **371,** 306–312 (1994).
13. Wood, B. A., Abbott, S. A. & Uyttershaut, H. Analysis of the dental morphology of Plio-Pleistocene hominids. IV. Mandibular postcanine root morphology. *J. Anat.* **156,** 107–139 (1988).
14. Senut, B., Pickford, M., Gommery, D., Mein, P. & Cheboi, K. First hominid from the Miocene (Lukeino Formation, Kenya). *C. R. Acad. Sci. Paris* **332,** 137–144 (2001).
15. Zollikofer, C. P. E. *et al.* Virtual cranial reconstruction of *Sahelanthropus tchadensis*. *Nature* doi: 10.1038/nature03397 (this issue).

Acknowledgements We thank the Chadian Authorities (Ministère de l'Éducation Nationale de l'Enseignement Supérieur et de la Recherche, Université de N'djaména, CNAR), the Ministère Français de l'Éducation Nationale (Faculté des Sciences, Université de Poitiers), the Ministère de la Recherche (CNRS: Département SDV & ECLIPSE), the Ministère des Affaires Étrangères (DCSUR, Paris and SCAC, N'Djamena) to the Région Poitou-Charentes, the American School of Prehistoric Research, the RHOI (co-Principal Investigators F. C. Howell and T. D. White), the Armée Française, MAM and Epervier for logistical support; the scanner staff of the University Museum, the University of Tokyo (microCT scanning, G. Suwa); to the ESRF, Grenoble (W. G. Stirling, General Director, A. Bravin and C. Nemoz, ID 17); many colleagues and friends for their help, especially G. Suwa for enamel thickness measurements, P. Tafforeau for ESRF three-dimensional scan reconstructions; T. D. White for discussions; all the other members of the Mission Paléoanthropologique Franco-Tchadienne (MPFT) who joined us for field missions; S. Riffaut and X. Valentin for technical support; and G. Florent and C. Noël for administrative guidance at the MPFT.

Competing interests statement The authors declare that they have no competing financial interests.

Correspondence and requests for materials should be addressed to M.B. (michel.brunet@univ-poitiers.fr).

Virtual cranial reconstruction of *Sahelanthropus tchadensis*

Christoph P. E. Zollikofer[1], Marcia S. Ponce de León[1], Daniel E. Lieberman[2], Franck Guy[2,3], David Pilbeam[2], Andossa Likius[4], Hassane T. Mackaye[4], Patrick Vignaud[3] & Michel Brunet[3]

[1]*Anthropologisches Institut/MultiMedia Laboratorium, Universität Zürich-Irchel, Winterthurerstrasse 190, 8057 Zürich, Switzerland*
[2]*Peabody Museum, Harvard University, 11 Divinity Avenue, Cambridge, Massachusetts 02138, USA*
[3]*Laboratoire de Géobiologie, Biochronologie et Paléontologie Humaine, CNRS UMR 6046, Faculté des Sciences, Université de Poitiers, 40 Avenue du Recteur Pineau, 86022 Poitiers Cedex, France*
[4]*Université de N'Djamena, BP 1117, N'Djamena, Tchad*

Previous research in Chad at the Toros-Menalla 266 fossiliferous locality (about 7 million years old) uncovered a nearly complete cranium (TM 266-01-60-1), three mandibular fragments and several isolated teeth attributed to *Sahelanthropus tchadensis*[1–3]. Of this material, the cranium is especially important for testing hypotheses about the systematics and behavioural characteristics of this species, but is partly distorted from fracturing, displacement and plastic deformation. Here we present a detailed virtual reconstruction of the TM 266 cranium that corrects these distortions. The reconstruction confirms that *S. tchadensis* is a hominid and is not more closely related to the African great apes[4,5]. Analysis of the basicranium further indicates that *S. tchadensis* might have been an upright biped, suggesting that bipedalism was present in the earliest known hominids, and probably arose soon after the divergence of the chimpanzee and human lineages.

Primary distortion in TM 266-01-60-1 results from morphological discontinuities along major cracks between the left and right sides of the face, between the supraorbital torus and the zygomatics, between the left and right posterior cranial vault including the nuchal plane and basioccipital, and along a coronally oriented crack between left frontal and temporoparietal portions of the vault (Fig. 1; also see Fig. 1 in ref. 1). However, anatomical continuity is well preserved in the sagittal and parasagittal planes, particularly between the face, the neurocranium and the basicranium. Anatomical continuity in the basicranium extends from the basisphenoid to the nuchal plane and within each of the cranial units delimited by major cracks, as evident from matching fracture lines between adjacent parts. Plastic deformation resulting in left–right asymmetry is noticeable in the maxilla. The fossil is barely affected by expanding matrix distortion[6], and no missing regions need to be estimated to reconstruct its original form.

A high-resolution computed tomography scan was used to create a digital representation of the TM 266 cranium that was disassembled along major cracks, cleaned of adhering matrix with the use of digital filtering, and then reconstructed virtually with two different established protocols (see Methods). The reconstruction, illustrated in Fig. 2, was evaluated with three independent tests. First, the face and neurobasicranial complex, which were reconstructed separately, fitted together at multiple points in an approximately coronal plane along the superior and lateral margins of the post-orbital region. Second, the reconstructed morphology was assessed a posteriori against an anatomical constraint not considered during the virtual reconstruction. In all mammals including primates, the posterior maxillary (PM) plane is approximately perpendicular relative to the neutral horizontal axis (NHA) of the orbits[7]. PM orientation was estimated by a plane that passes, in lateral projection, from the maxillary tuberosities through the pterygopalatine fossae[8]. In the TM 266 reconstruction, this plane is about 89° relative to the NHA (estimated from the orbital margins and the partly preserved medial walls). As a third test, the TM 266 reconstruction was compared with three-dimensional shape variability in a comparative African ape/fossil hominid sample (see Methods). We performed a generalized least-squares superimposition[9] of the symmetrized landmark configurations[10] of all specimens and calculated the minimum form change necessary to transform the TM 266 reconstruction to the closest possible hypothetical *Pan* and *Gorilla* cranial forms with the use of the 99% probability density borders as a minimum-distance criterion (Fig. 3). Figure 3a–c shows this procedure for the first three PCs, which account for more than 58% of the total shape variability. To account for allometric shape effects, all shape PCs were regressed against centroid size to obtain a common allometric shape score[11] (Fig. 3d). The isolated fragments of the TM 266 cranium were then positioned to fit the calculated three-dimensional landmark configurations of the closest-possible *Pan* and *Gorilla* shapes (Fig. 3e). The resulting '*Pan*-like' and '*Gorilla*-like' morphologies are anatomically infeasible, involving overlap between neurocranial fragments and disruption of anatomical continuity between neighbouring facial fragments. Although the cranial morphology of TM 266-01-60-1 cannot be reconstructed to fall within the size–shape

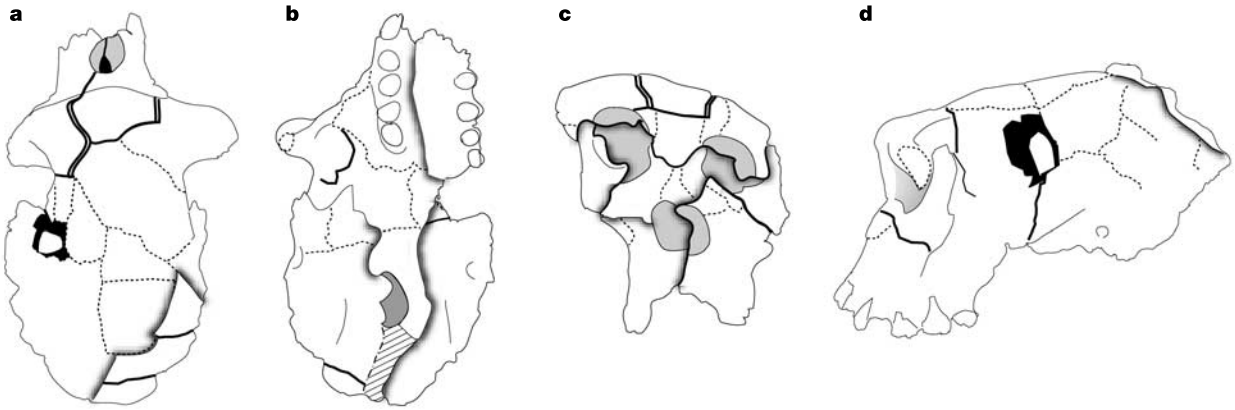

Figure 1 State of preservation of the unreconstructed TM 266 cranium. **a**, Superior view. **b**, Inferior view. **c**, Frontal view. **d**, Left lateral view. Thin lines and grey areas indicate anatomical structures; shadowed lines, superposition of cranial parts resulting from postmortem distortion; bold lines, major cracks (double lines, disruption of anatomical continuity); stippled lines, matching fracture lines between electronically isolated components; black areas, missing parts or matrix filling. Note that the everted occipital fragment (hatched area in **b**) obscures the original morphology and orientation of the nuchal plane.

space of known African ape morphologies, it is within the size–shape space defined by other Pliocene hominids.

The reconstruction in Fig. 2 is therefore a robust estimate of the cranial form of TM 266-01-60-1 that supports most of the details originally described[1,2]. However, several features differ notably from those of the original specimen: the cranium as a whole is wider, the occipital contour is rounder sagittally, the nuchal plane is oriented more horizontally, the orbits are larger and more circular, and the face is superoinferiorly taller (additional standard craniometric measurements are provided in Supplementary Table 1). The changes evident in the TM 266 reconstruction highlight its unique morphology and confirm several derived features shared with later hominids such as a relatively vertical face with an anteroposteriorly short premaxilla; an anteriorly-positioned foramen magnum linked to a relatively short basioccipital; a relatively flat, large, and horizontally-oriented nuchal plane; and downward lipping of the nuchal crest[12–14]. These features, together with other dental features (see refs 1, 2), support the conclusion that *Sahelanthropus* is a hominid (*contra* Wolpoff *et al.*[4,5]).

Finally, the TM 266 reconstruction permits an assessment of the hypothesis that *Sahelanthropus* was a biped, an important feature of Pliocene hominids and possibly several Late Miocene hominids[15,16]. Unequivocal evidence for bipedalism is difficult to obtain from the cranium, but several lines of evidence suggest that TM 266-01-60-1

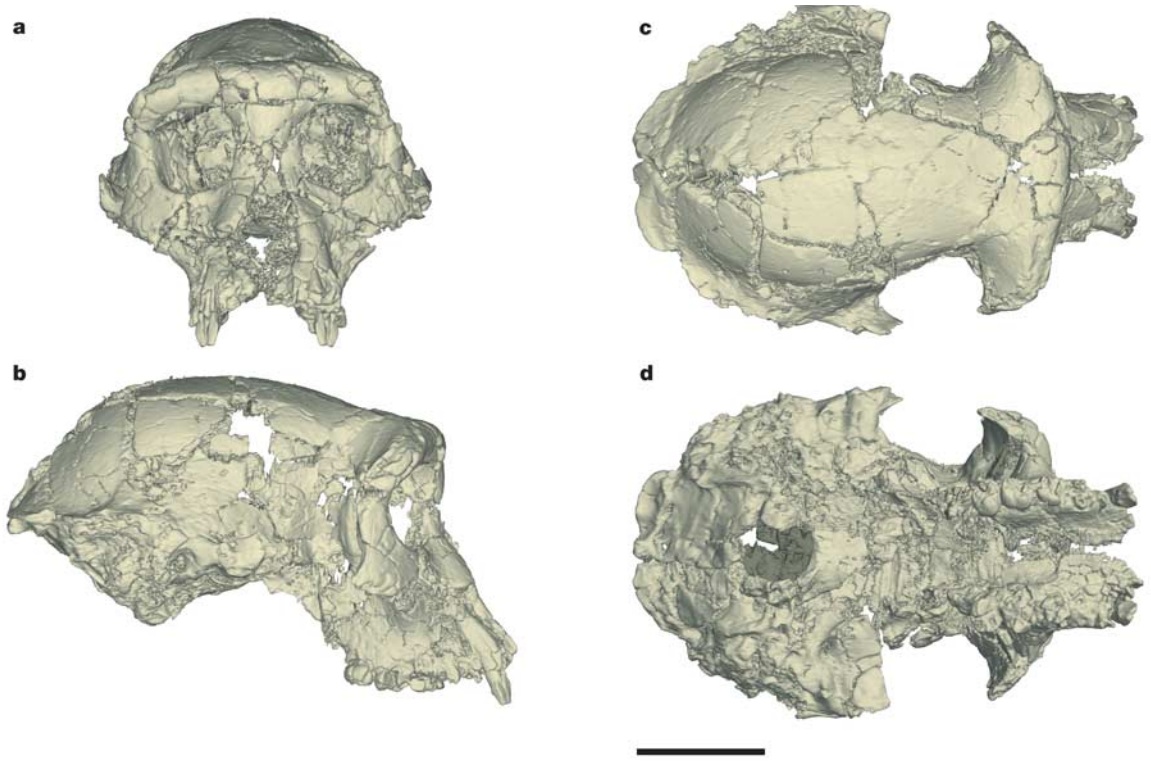

Figure 2 Virtual reconstruction of the TM 266 cranium (Frankfurt Horizontal plane orientation, orthographic projection). **a**, Frontal view. **b**, Right lateral view. **c**, Superior view. **d**, Inferior view. Scale bar, 5 cm.

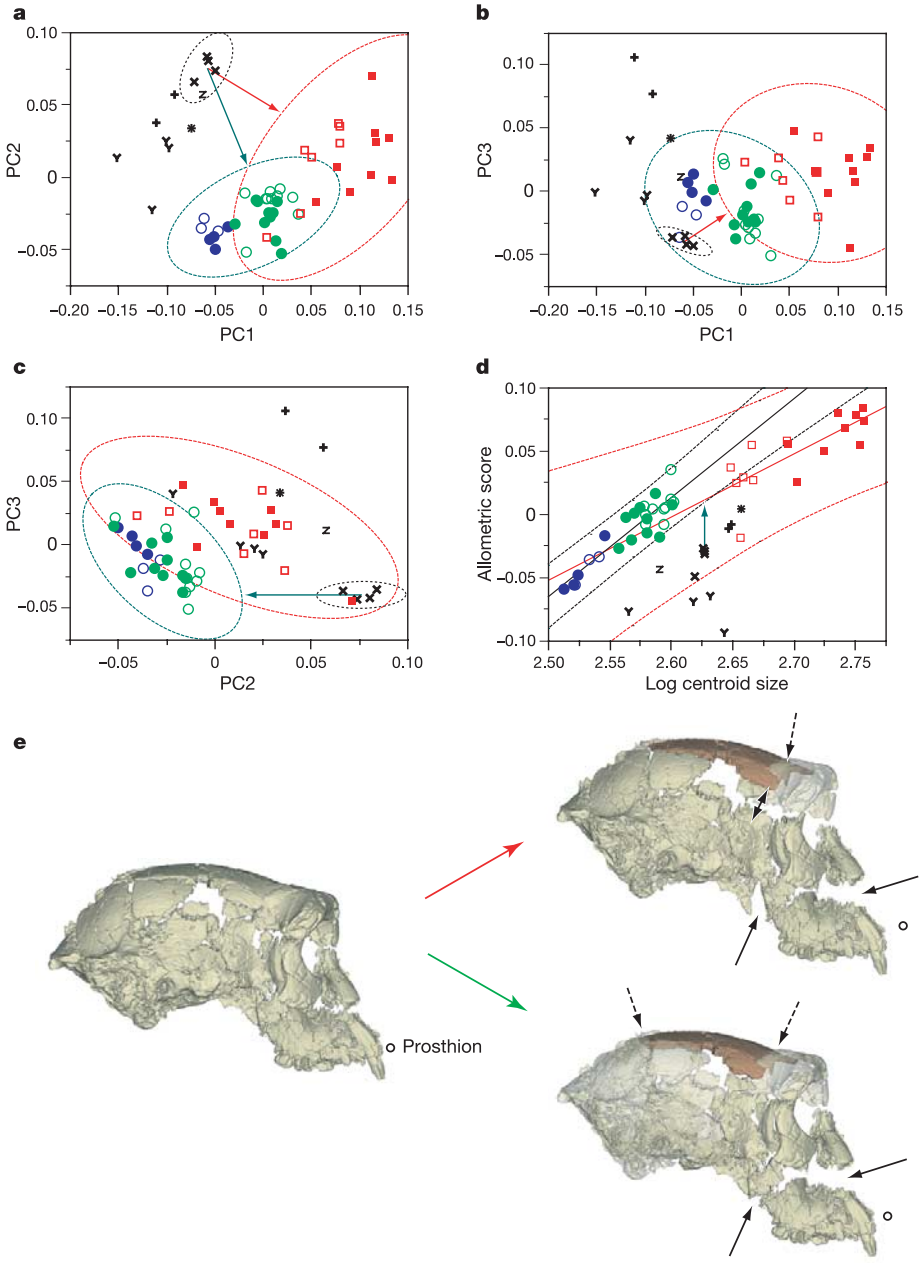

Figure 3 TM 266 cranial reconstruction and comparative fossil hominid/African ape morphology. **a**–**d**, Evaluation of size-adjusted minimum distance between TM 266-01-60-1 and the African apes with data scatter in size–shape space defined by PCs1-3. Variance proportions: PC1, 39.1%; PC2, 11.3%; PC3, 8.3%. X, reconstructed variants of TM 266-01-60-1; Y, fossil *Homo*; Z, *Australopithecus africanus*; stars, *A. afarensis*; plus signs, *Paranthropus*; blue circles, *Pan paniscus*; green circles, *Pan troglodytes*; squares, *Gorilla gorilla* (open symbols, females; filled symbols, males). Stippled lines indicate 99% probability densities for *Pan*, *Gorilla* and TM 266-01-60-1 reconstructions. **e**, Transformation of TM 266-01-60-1 into hypothetical closest African ape morphologies in multidimensional size–shape space: green arrows, transformation into *Pan*; red arrows, transformation into *Gorilla*; black arrows indicate resulting disruption (solid) and overlap (dashed) between neighbouring fragments.

might have been bipedal. Despite substantial differences in neck orientation, humans and non-human primates tend to locomote with their orbital planes (the line joining the superior and inferior margins of the orbits) approximately perpendicular to the ground[17]. In addition, primates orient the upper cervical vertebrae approximately perpendicular to the plane of the foramen magnum, and with only a limited range (about 10°) of flexion and extension possible at the cranio-cervical joint[18]. The combined effect of these angular constraints is that the angle between the foramen magnum and the orbital plane (Fig. 4) is nearly perpendicular in *Homo sapiens* ($103.2 \pm 6.9°$, $n = 23$) but more acutely angled in *Pan troglodytes* ($63.7 \pm 6.2°$, $n = 20$), and other species with more pronograde postures. The foramen magnum angle relative to the orbital plane in the TM 266 reconstruction is 95°, similar to that in humans and later bipedal hominids such as *Australopithecus afarensis* (AL 444-2) and *A. africanus* (Sts 5)[13,17]. TM 266-01-60-1 as a quadruped would require an unusually extended angle of the neck relative to the plane of the foramen magnum.

Although increases in brain volume relative to cranial base length have been implicated in horizontal rotation of the posterior cranial base[19], such an explanation is unlikely for the TM 266 cranium

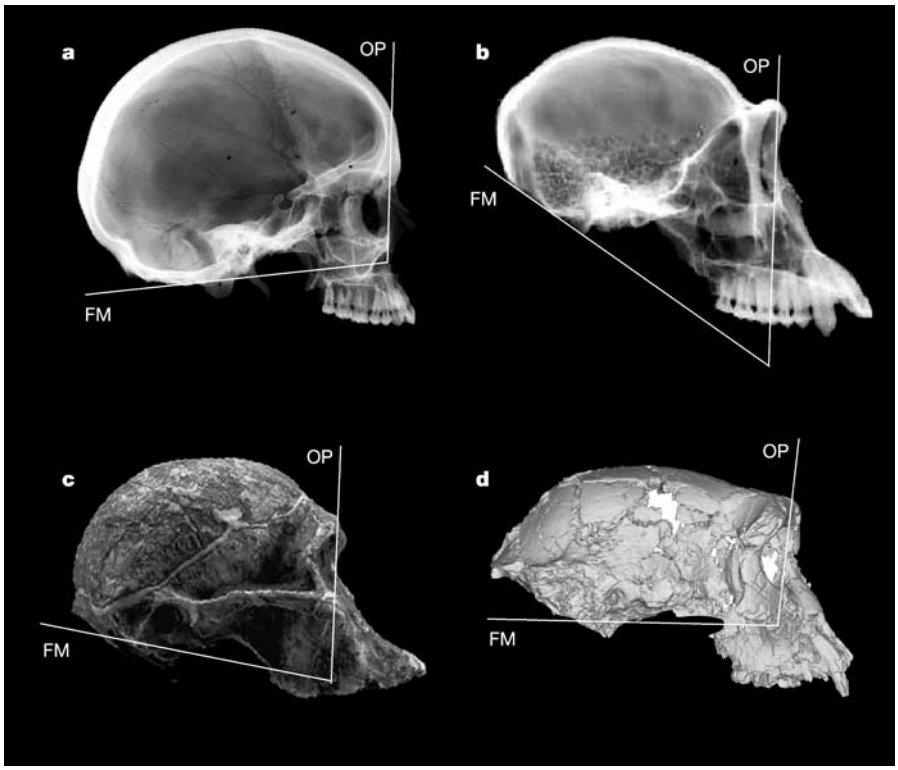

Figure 4 Angular relationship between foramen magnum (FM) and orbital (OP) planes. **a**, *Homo sapiens*; **b**, *Pan troglodytes*; **c**, *Australopithecus africanus* (Sts 5); **d**, TM 266 reconstruction.

whose estimated endocranial volume, 360–370 ml, is the smallest yet documented for an adult hominid but is within the range in chimpanzees[20]. Another related indication of bipedality in *S. tchadensis* is the flat nuchal plane oriented at about 36° relative to the Frankfurt Horizontal, well within the range of *Australopithecus* and *Homo* but not *Pan*[21]. In addition, the nuchal crest of the TM 266 cranium has downward lipping, a feature present in other bipedal hominids (for example AL 444-2, OH 5) but not in *Pan* or *Gorilla*. However, postcranial evidence will be necessary to test more rigorously the hypothesis that *S. tchadensis*—the earliest known hominid, found 2,600 km west of the East African rift valley—was a biped. □

Methods

Data acquisition and state of preservation

The TM 266-01-60-1 original was scanned with an Industrial Systems CT scanner (tube voltage 450 kV, tube current 5 mA, beam collimation 0.4 mm, interslice distance 0.4 mm, pixel size 0.2 mm × 0.2 mm, pixel depth 16 bits). The virtual cranium was disassembled along major cracks, and matrix filling was removed from endocranial and paranasal cavities with the use of interactive data segmentation tools[22]. Virtual separation of cranial fragments revealed substantial overlap between right and left sides of the cranium from post-mortem compression, causing an elongated appearance of the vault in superior view (see figure 1c in ref. 1). In addition, the lower face and orbital margins are shifted left and superiorly relative to the supraorbital torus and zygomatic processes of the frontal (Fig. 1c), the basioccipital is shifted towards the left petrosal (Fig. 1b), and the right posterior cranial vault and nuchal plane overlay the left side (Fig. 1a, b), altering the true orientation of the nuchal plane in the sagittal plane (see figure 1b in ref. 1). The exposed borders of parts of the cranial vault and palate are partly eroded; the mastoids and petrosal portions of the temporal bones also suffered some surface damage but are undistorted, as evinced by the mirror-symmetric position of the well-preserved left and right inner ear cavities relative to features such as the external acoustic meatus and the stylomastoid foramen. The left temporal fossa is partly missing, but corresponding structures on the right side are well preserved.

Virtual three-dimensional reconstruction

The reconstruction of the cranium followed established methods[23,24]. Once partitioned, isolated fragments were repositioned and reoriented in virtual space to restore morphological continuity along fractures, sutures and other anatomical features within and between bones. The cranium was independently reconstructed four times by two of us (M.S.P.L. and C.P.E.Z.), each using two different protocols. Protocol A used features shared by all mammal crania to position and orient each fragment. First, the basioccipital was positioned and oriented in the midsagittal plane. The temporals were then adjoined from both sides and aligned by placing all of the left and right semicircular canals in approximately parallel orientation[25,26]. Lateral and superior parts of the vault were adjoined by using the well-preserved temporal lines to establish bilateral symmetry. Within the face, displaced but undistorted portions of the supraorbital torus and orbital margins were repositioned symmetrically relative to the midsagittal plane. Left–right asymmetry in the maxilla from plastic taphonomic deformation was partly corrected with the use of published methods[24]. Protocol B used a geometric approach based on stepwise reduction of degrees of freedom of the position and orientation of individual parts relative to each other. This method takes advantage of the almost complete preservation of the TM 266 cranium, in which the position and orientation of each fragment is spatially constrained by contacts with all neighbouring fragments, and overall morphology is constrained by bilateral symmetry. Translational degrees of freedom were first reduced by re-establishing morphological continuity between dislocated fragments along matching fracture lines (along the nuchal plane, along cracks in the right parietal, between parts of the supraorbital torus, and between dislocated parts of the midface). Rotational degrees of freedom between adjacent fragments were then reduced by stepwise integration of fragments into the reconstruction, followed by iterative adjustments until a symmetrical integrated morphology was achieved. These procedures were applied to orient left and right neurobasicranial sides relative to each other, and the maxillae relative to the midface. Last, deviations from bilateral symmetry in the maxilla were partly corrected as in protocol A.

In both protocols, the face and the braincase were reconstructed independently and then assembled by using anatomical continuities within the squamous portions of the frontal; along preserved continuities between the basisphenoid, the pterygoid processes and the right side maxillary tuberosity; and between the bones of the right temporal fossa (squamous sphenoid, zygomatic, maxilla and frontal). Differences between the four reconstructions, as visualized in shape space, are comparatively small (Fig. 3a–c) and reflect inter-observer and inter-protocol disparity. Major variations concern maxillary width measured at M^2 ($\pm$0.9 mm); foramen magnum height relative to porion ($\pm$1.1 mm); and facial orientation relative to the braincase, as measured by the angle between nasion–basion and nasion–prosthion ($\pm$2.3°). Figure 2 shows the final result, obtained by averaging all four reconstructions.

Geometric morphometric analysis

The analysis included adult crania of 16 *G. gorilla* (9 males, 7 females), 20 *P. troglodytes* (10 males, 10 females), 7 *P. paniscus* (4 males, 3 females) and 8 fossil hominids (casts of ER1813, ER1470, ER3733, KNM-WT 15000, STS5, OH5, ER406 and virtual reconstruction of AL444-2). All primate specimens are from the A. H. Schultz Collection,

University of Zurich, the Peabody Museum, Harvard University, and the Royal Africa Museum, Tervuren. Midsagittal landmarks used were nasion, glabella, bregma, lambda, inion, opisthion, basion, sphenobasion, staphylion, prosthion and nasospinale; paired landmarks (left and right sides taken when possible) were maxillofrontale, supraorbitale, orbitale, frontomalare orbitale, zygomaxillare, jugale, foramen infraorbitale, M^2 most buccal point, foramen stylomastoideum, foramen caroticum, foramen ovale, asterion, porion and pterion.

Received 17 September 2004; accepted 25 January 2005; doi:10.1038/nature03397.

1. Brunet, M. *et al.* A new hominid from the Upper Miocene of Chad, Central Africa. *Nature* **418,** 145–151 (2002).
2. Brunet, M. *et al.* New material of the earliest hominid from the Upper Miocene of Chad. *Nature* doi:10.1038/nature03392 (this issue).
3. Vignaud, P. *et al.* Geology and palaeontology of the Upper Miocene Toros-Menalla hominid locality, Chad. *Nature* **418,** 152–155 (2002).
4. Wolpoff, M. H., Senut, B., Pickford, M. & Hawks, J. *Sahelanthropus* or '*Sahelpithecus*'? *Nature* **419,** 581–582 (2002).
5. Brunet, M. *et al. Sahelanthropus* or '*Sahelpithecus*'? (Reply). *Nature* **419,** 582 (2002).
6. White, T. Early hominids—diversity or distortion? *Science* **299,** 1994–1997 (2003).
7. McCarthy, R. C. & Lieberman, D. E. Posterior maxillary (PM) plane and anterior cranial architecture in primates. *Anat. Rec.* **264,** 247–260 (2001).
8. Enlow, D. H. *Facial Growth* (Saunders, Philadelphia, 1990).
9. Rohlf, F. J. & Slice, D. Extensions of the Procrustes method for the optimal superimposition of landmarks. *Syst. Zool.* **39,** 40–59 (1990).
10. Zollikofer, C. P. E. & Ponce de León, M. S. Visualizing patterns of craniofacial shape variation in *Homo sapiens*. *Proc. R. Soc. Lond. B* **269,** 801–807 (2002).
11. Penin, X., Berge, C. & Baylac, M. Ontogenetic study of the skull in modern humans and the common chimpanzees: neotenic hypothesis reconsidered with a tridimensional Procrustes analysis. *Am. J. Phys. Anthropol.* **118,** 50–62 (2002).
12. Aiello, L. & Dean, C. *An Introduction to Human Evolutionary Anatomy* (Academic, London, 1990).
13. Kimbel, W. H., Johanson, D. & Rak, Y. *The Skull of Australopithecus afarensis* (Oxford Univ. Press, New York, 2004).
14. Wood, B. & Richmond, B. G. Human evolution: taxonomy and paleobiology. *J. Anat.* **196,** 19–60 (2000).
15. Haile-Selassie, Y. Late Miocene hominids from the Middle Awash, Ethiopia. *Nature* **412,** 178–181 (2001).
16. Pickford, M., Senut, B., Gommery, D. & Treil, J. Bipedalism in *Orrorin tugenensis* revealed by its femora. *C. R. Palevol.* **1,** 191–203 (2002).
17. Strait, D. S. & Ross, C. F. Kinematic data on primate head and neck posture: implications for the evolution of basicranial flexion and an evaluation of registration planes used in paleoanthropology. *Am. J. Phys. Anthropol.* **108,** 205–222 (1999).
18. Graf, W., de Waele, C. & Vidal, P. P. Functional anatomy of the head–neck movement system of quadrupedal and bipedal mammals. *J. Anat.* **186,** 55–74 (1995).
19. Lieberman, D. E., Ross, C. F. & Ravosa, M. J. The primate cranial base: ontogeny, function, and integration. *Yb. Phys. Anthropol.* **43,** 117–169 (2000).
20. Holloway, R. L., Broadfield, D. C., Yuan, M. S., Schwartz, J. H. & Tattersall, I. *The Human Fossil Record Vol. 4: Brain Endocasts* (Wiley, New York, 2004).
21. Kimbel, W. H., White, T. D. & Johanson, D. C. Cranial morphology of *Australopithecus afarensis*: a comparative study based on a composite reconstruction of the adult skull. *Am. J. Phys. Anthropol.* **64,** 337–388 (1984).
22. Gonzalez, R. C. & Woods, R. E. *Digital Image Processing* (Prentice Hall, Upper Saddle River, New Jersey, 2002).
23. Zollikofer, C. P. E., Ponce de León, M. S. & Martin, R. D. Computer-assisted paleoanthropology. *Evol. Anthropol.* **6,** 41–54 (1998).
24. Ponce de León, M. S. & Zollikofer, C. P. E. New evidence from Le Moustier. 1: Computer-assisted reconstruction and morphometry of the skull. *Anat. Rec.* **254,** 474–489 (1999).
25. Delattre, A. & Fenart, R. *L'hominisation du Crâne Étudiée par la Méthode Vestibulaire* (CNRS, Paris, 1960).
26. Zollikofer, C. P. E., Ponce de León, M. S., Martin, R. D. & Stucki, P. Neanderthal computer skulls. *Nature* **375,** 283–285 (1995).

Supplementary Information accompanies the paper on **www.nature.com/nature**.

Acknowledgements We thank the Chadian Authorities (Ministère de l'Éducation Nationale de l'Enseignement Supérieur et de la Recherche, Université de N'Djaména, Centre National d'Appui à la Recherche au Tchad), the Ministère Français de l'Éducation Nationale (Faculté des Sciences, Université de Poitiers), Ministère de la Recherche (CNRS: Département SDV & ECLIPSE), Ministère des Affaires Étrangères (DCSUR Commission des fouilles, Paris, et SCAC Ambassade de France à N'Djaména), the Revealing Hominid Origins Initiative (co-principal investigators F. C. Howell and T. D. White), the American School of Prehistoric Research, Harvard University, and the Swiss National Science Foundation, for support; the MultiMedia Laboratorium, University of Zürich (P. Stucki); EMPA Dübendorf, Switzerland, for industrial computed tomography (A. Flisch); all the MPFT members; and S. Riffaut, X. Valentin, G. Florent and C. Noël for technical support and administrative guidance.

Competing interests statement The authors declare that they have no competing financial interests.

Correspondence and requests for materials should be addressed to M.B. (michel.brunet@univ-poitiers.fr).

Evolutionary diversification of TTX-resistant sodium channels in a predator–prey interaction

Shana L. Geffeney[1], Esther Fujimoto[1]*, Edmund D. Brodie III[2], Edmund D. Brodie Jr[1] & Peter C. Ruben[1]

[1]*Department of Biology, Utah State University, Logan, Utah 84322-5305, USA*
[2]*Department of Biology, Indiana University, Bloomington, Indiana 47405-3700, USA*

* Present address: Department of Neurobiology and Anatomy, University of Utah School of Medicine, Salt Lake City, Utah 84123-3401, USA

Understanding the molecular genetic basis of adaptations provides incomparable insight into the genetic mechanisms by which evolutionary diversification takes place. Whether the evolution of common traits in different lineages proceeds by similar or unique mutations, and the degree to which phenotypic evolution is controlled by changes in gene regulation as opposed to gene function, are fundamental questions in evolutionary biology that require such an understanding of genetic mechanisms[1–3]. Here we identify novel changes in the molecular structure of a sodium channel expressed in snake skeletal muscle, $tsNa_V1.4$, that are responsible for differences in tetrodotoxin (TTX) resistance among garter snake populations coevolving with toxic newts[4]. By the functional expression of $tsNa_V1.4$, we show how differences in the amino-acid sequence of the channel affect TTX binding and impart different levels of resistance in four snake populations. These results indicate that the evolution of a physiological trait has occurred through a series of unique functional changes in a gene that is otherwise highly conserved among vertebrates.

Identifying the connection between genotype and phenotype is the critical step uniting evolutionary studies of phenotypic diversity with more proximate investigations of development, function and structure[5–8]. One emerging picture is that the process of adaptive radiation might be more predictable at the genetic level than previously imagined and that the regulation of genes of major effect rather than the alteration of functional products might explain much phenotypic diversity[1,3]. Identifying the genetic basis of bill differences in Galapagos finches[6] and eyespot patterns in butterflies[5], and the loss of pelvic spines in sticklebacks[7] or eyes in cave-dwelling fish[8], has led to an increased understanding about how evolution generates convergent and divergent traits at the molecular level. In each of these cases, ecologically important morphological differences between lineages are explainable through changes in the regulation of single genes in developing tissues. However, functional changes in the protein-coding regions of structural genes explain adaptive differences in other cases, including cryptic pigmentation in rodents[9] and pesticide resistance in insects[10].

Coevolution between the garter snake *Thamnophis sirtalis* and its toxic prey, the newt *Taricha granulosa*, has resulted in geographic variability in a physiological trait, resistance to TTX in predator lineages[4]. Tetrodotoxin causes paralysis and death by binding to the outer pore of voltage-gated sodium channels and blocking nerve and muscle fibre activity[11]. Some populations of *Taricha* have extremely high levels of TTX in their skin that provide an almost impenetrable defence against predators[12], yet elevated TTX resistance has evolved at least twice within the radiation of *T. sirtalis*[4,13]. This physiological adaptation is at least partly accounted for by the expression of TTX-resistant sodium channels in the skeletal muscle of resistant garter snakes[14]. Here we identify the molecular mechanisms underlying this diversification.

The extent to which TTX affects nerve and muscle tissue is